UNCLASSIFIED

AD NUMBER
AD852114
NEW LIMITATION CHANGE
TO Approved for public release, distribution unlimited
FROM Distribution authorized to U.S. Gov't. agencies and their contractors; Critical Technology; JUL 1968. Other requests shall be referred to Air Force Armament Laboratory, Attn: ATBR, Egling AFB, FL 32542.
AUTHORITY
AFATL ltr, 8 Mar 1977

THIS PAGE IS UNCLASSIFIED

AFATL-TR-68-82

FLIGHT DYNAMICS OF THE BASIC FINNER

IN VARIOUS DEGREES OF FREEDOM

John D. Nicolaides
Robert S. Eikenberry
Charles W. Ingram
Thomas A. Clare

Department of Aero-Space Engineering
University of Notre Dame

D D C

MAY 19 1969

B

FLIGHT DYNAMICS OF THE BASIC FINNER
IN VARIOUS DEGREES OF FREEDOM

John D. Nicolaides
Robert S. Eikenberry
Charles W. Ingram
Thomas A. Clare

FOREWORD

This report contains theoretical and experimental information on the Basic Finner program. The work was carried out during the period Feb 1966 to May 1968 under the direction of Dr. John D. Nicolaides, Chairman of the Aero-Space Engineering Department, University of Notre Dame. This study was authorized under Contract AF 08(635)-5275 by the Air Force Armament Laboratory, Eglin Air Force Base, Florida. Program monitor for the Armament Laboratory was Mr. C. B. Butler (ATBR).

Information in this report is embargoed under the Department of State International Traffic In Arms Regulations. This report may be released to foreign governments by departments or agencies of the U. S. Government subject to approval of the Air Force Armament Laboratory (ATBR), Eglin AFB, Florida 32542, or higher authority within the Department of the Air Force. Private individuals or firms require a Department of State export license.

This technical report has been reviewed and is approved.

JOSEPH E. DUVAL, Colonel, USAF
Chief, Ballistics Division

ABSTRACT

Basic Finner models are tested in both horizontal and vertical wind tunnels in order to develop dynamic testing techniques and to perfect new methods of non-linear analysis. The simple free motions of pure pitching and pure rolling are first studied. Then, free angular motions of combined pitching, yawing, and rolling are investigated. While the linear analysis methods appear to yield good results, the new non-linear analysis methods are found to be essential in providing an accurate representation of the various motions and in providing correct values for the various static and dynamic stability coefficients.

iii

(The reverse of this page is blank)

TABLE OF CONTENTS

LIST OF FIGURES

LIST OF SYMBOLS

p, q, r	Missile angular velocity in space, rad/sec
U, V, W	Missile velocity in space, ft/sec
$\bar{\alpha}$	Complex angle of attack,
α	Angle of attack
β	Angle of Side Slip
d	Reference length = Missile Diameter, ft.
S	Reference area =
m	Missile Mass, slugs
V	Total velocity, ft/sec
ρ	Density, slugs/ft^3
I	Transverse Moment of Inertia, slug-ft^2
I_x	Axial Moment of Inertia, slug-ft^2
Q	Dynamic pressure = $\frac{1}{2}\rho V^2$, lb/ft^2
S	Ballistic Gyroscopic Stability Factor
$\omega_{1,2}$	Nutation and Precession frequencies, rad/sec
$\lambda_{1,2}$	Nutation and Precession damping, factors
$K_{1,2,-4}$	Arms of the Quadricyclic Theory
γ	Roll Orientation Angle with Respect to the Plane of Angle of Attack
α_T	Trim Angle
$C_{M\alpha}$	Static Moment Stability Coefficient

$$C_{M\alpha} = \frac{M_\alpha \alpha}{\bar{\alpha} Q S d} = C_{m\alpha} = -C_{n\beta}$$

LIST OF SYMBOLS (concluded)

C_{Mq} **Damping Moment Stability Coefficient**

$$C_{Mq} = \frac{M_q q}{\left(\frac{qd}{2V}\right) QSd} = C_{mq} = -C_{n_r}$$

$C_{M\dot{\alpha}}$ **Lag Moment Stability Coefficient**

$$C_{M\dot{\alpha}} = \frac{M_{\dot{\alpha}} \dot{\alpha}}{\left(\frac{\dot{\alpha}d}{2V}\right) QSd} = C_{m\dot{\alpha}} = -C_{n\dot{\beta}}$$

$C_{MP\alpha}$ **Magnus Moment Stability Coefficient**

$$C_{MP\alpha} = \frac{M_{P\alpha} P\alpha}{\alpha \left(\frac{Pd}{2V}\right) QSd} = C_{mP\beta} = -C_{nP\alpha}$$

C_{lp} **Roll Damping Moment Stability Coefficient**

$$C_{lp} = \frac{L_p P}{\left(\frac{Pd}{2V}\right) QSd}$$

$C_l(\alpha)$ **Induced Roll Moment Coefficient**

$$C_l(\alpha) = \frac{L(\alpha)}{QSd \; \sin 4\gamma}$$

$$C_{l\gamma\alpha} = \left. \frac{\delta C_l(\alpha)}{\delta \gamma} \right|_{\gamma = \gamma_r}$$

For additional information, see Reference 3.

SECTION I

INTRODUCTION

The Basic Finner was designed as a fundamental research configuration for unguided finned missiles following World War II.[1,2] Numerous studies have been carried out in air and in water. The air tests have utilized both wind tunnels and aeroballistic ranges over the entire speed range, subsonic, transonic, supersonic, and hypersonic. In water, tests have utilized towing tanks, rotating arms, water tunnels, and free drops. Unfortunately, the static and dynamic stability coefficients obtained from the various testing techniques and facilities do not always agree. Serious unexplained differences persist.

There is a fundamental requirement to obtain correct values for the various stability coefficients in order to understand and predict actual missile performance and accuracy. Therefore the introduction of a basic research program to develop wind tunnel dynamic testing techniques and to perfect methods of non-linear data analysis was initiated.[18]

The Basic Finner is first tested by allowing free yawing motion about a side support in a horizontal wind tunnel. The resulting angular position data is reduced both by a linear method of data analysis[3] and by a new method of non-linear analysis.

A unique vertical wind tunnel is used in the studies of the free rolling motion of the Basic Finner mounted on a rear sting support. Again, both linear and non-linear methods of analysis are employed. In these studies particular attention is directed towards the determination of the non-linear induced roll moment coefficient, $C_\ell(\alpha)$, which can cause Roll Lock-In and which is a requirement for Catastrophic Yaw.

Special emphasis is placed on testing techniques which permit complete model motions in all three degrees of angular freedom. In one testing technique the Basic Finner is mounted on a side support in a horizontal wind tunnel. The model is free to pitch, yaw, and roll, except for a small central section which does not roll. In another 3-D testing technique the model is mounted on a rear sting in a vertical downdraft wind tunnel.

In all cases the non-linear methods of analysis are first studied by using data generated on a high speed computer by numerical integration of the exact equations of motion. The results obtained by applying the non-linear analysis methods to this computer data are compared with the known computer inputs. The non-linear analysis methods are then applied to various dynamic wind tunnel data.

1

In these studies particular attention is given to non-linearities in the static moment coefficient, C_{M_α} the damping and lag moment coefficients, $C_{M_q} + C_{M_{\dot\alpha}}$ and the Magnus moment coefficient, $C_{M_{p\alpha}}$.

SECTION II

GENERAL METHOD OF ANALYSIS

In general, the various free motions of a missile are described by an equation of the form

$$\alpha(T) = Ke^{(\lambda + i\omega)t} + a_T \tag{1}$$

It is desired to "fit" this equation to experimental data. The above equation, however, is non-linear in the unknowns ω and λ; therefore the conventional method of least squares cannot be used.

The left side of Equation (1) may be expressed in terms of the experimental data as $\alpha(T) + v$, where v is the residual (the difference between the calculated point and the data point). Equation (1) now becomes,

$$\alpha(t) + V = f(t, a_T, K, \lambda, \omega, \delta) \tag{2}$$

The five unknowns may be expressed as,

$$a_T = a_{T_o} + \Delta a_T$$

$$K = K_o + \Delta K$$

$$\lambda = \lambda_o + \Delta \lambda$$

$$\omega = \omega_o + \Delta \omega$$

$$\delta = \delta_o + \Delta \delta$$

where a_{T_o}, K_o, λ_o, etc. are initial approximations. Equation 2 now becomes

$$\alpha(t) + V = f(t, a_{T_o} + \Delta a_T, K_o + \Delta K, \lambda_o + \Delta \lambda, \omega_o + \Delta \omega, \delta_o + \Delta \delta) \tag{3}$$

3

Expansion of Equation (3) in a Taylor Series gives,

$$a(t) + V = f(t, \alpha_{T_o}, K_o, \lambda_o, \omega_o, \delta_o) + \Delta\alpha_T \frac{\partial f}{\partial \alpha_{T_o}} + \Delta K \frac{\partial f}{\partial K_o}$$

$$+ \Delta\lambda \frac{\partial f}{\partial \lambda_o} + \Delta\omega \frac{\partial f}{\partial \omega_o} + \Delta\delta \frac{\partial f}{\partial \delta_o}$$

(4)

If the initial approximations are good, the $\triangle$ terms will be small and the higher order terms may be neglected. Equation (4) is then linear in the differential corrections $\triangle\alpha_T, \triangle K, \ldots$ and least squares methods can be applied to their determination. Once the differential corrections are determined they may be added to the initial estimates of the unknowns α_{T_o}, K_o, λ_o, ... and the process may be repeated to determine a new set of differential corrections. This Method of Differential Corrections is repeated until the sum of the squares of the residuals is a minimum or until there is no significant change in the unknowns.

The Wobble computer program[4] employs the Method of Differential Corrections (MDC) as described above to fit the solutions of the governing differential equations of motion to experimental angular data. This program is equipped to fit the simple equation, Equation (1), or the more complex solution for the Quadricyclic Theory

$$\vec{a} = K_1 e^{(\lambda_1 + i\omega_1)t} + K_2 e^{(\lambda_2 + i\omega_2)t} + K_3 e^{ipt} + K_4$$

(5)

By overlapping fits of small sections of data the motion parameters can be determined as continuous functions of time. The various aerodynamic stability coefficients may then be determined from these parameters.

4

SECTION III

ONE DEGREE OF FREEDOM PITCHING MOTION

A Basic Finner model was mounted on a side support in a horizontal wind tunnel and allowed to freely yaw. A schematic of the Basic Finner is shown in Figure 1.
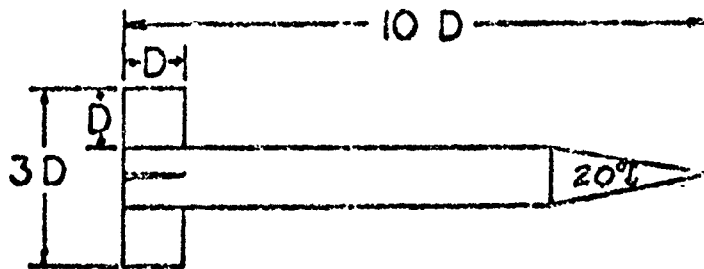
Figure 1. Schematic of Basic Finner

In one case ball bearings were used. In a more optimum case, the model was supported from below by a needle resting in a sapphire jewel cup. These tests were all conducted at low subsonic speeds.

Linear Analysis

The differential equation for one degree of freedom pitching motion may be written as[3]

$$M_\alpha \alpha + M_q q + M_{\dot\alpha}\dot\alpha + M_{\delta_E}\delta_E = I\dot{q} \quad , \qquad \dot\alpha = q \tag{6}$$

or

$$\ddot\alpha + N_1\dot\alpha + N_2\alpha = N_3 \tag{7}$$

The general solution, when the coefficients are constants, is given by

$$\alpha = K_1 e^{(\lambda_1 + i\omega_1)t} + K_2 e^{(\lambda_2 + i\omega_2)t} + K_3 \tag{8}$$

since $\omega_1 = -\omega_2$ and $\lambda_1 = \lambda_2$, this may be simplified to

5

$$a = a_T + Ke^{\lambda t}\cos(\omega t + \delta) \tag{9}$$

where

$$\lambda_{1,2} + i\omega_{1,2} = -\frac{N_1}{2} \pm \frac{1}{2}\sqrt{N_1^2 - 4N_2} \tag{10}$$

$$C_{M\alpha} \approx -\frac{2I\omega^2}{\rho U^2 SD} \tag{11}$$

$$C_{Mq} + C_{M\dot{\alpha}} \approx \frac{8I\lambda}{\rho USD} \tag{12}$$

The purpose of this analysis was to measure precisely the angle of attack, $\overline{\alpha}$, as a function of time and to use Equation (9) to obtain ω and λ , and then use Equations (11) and (12) to obtain $_{M\alpha}$ and $(C_{Mq} + C_{M\dot{\alpha}})$.

It was also desired to test the transformation equations for the stability coefficients using six different center of gravity positions. Once the moment stability coefficients, $C_{M\alpha}$ and $(C_{Mq} + C_{M\dot{\alpha}})$ have been measured at one center of gravity, the axis of rotation may be changed and new values obtained for each of the six positions on the Basic Finner model.

The equations which relate the stability coefficients at one center of gravity (or rotation axis) to another center of gravity are[3]

$$C_{M\alpha}^{*} = C_{M\alpha_0} + C_{Z\alpha}\left(\frac{X_0}{D}\right) \tag{13}$$

$$C_{Mq}^{*} - 2\left(\frac{X_0}{D}\right)C_{M\alpha}^{*} = C_{Mq} + \left(\frac{X_0}{D}\right)C_{Z_q} \tag{14}$$

The sign convention for the forces and moments discussed above are shown in Figure 2.

A model of the Basic Finner was mounted on precision bearing on a side support.[5,6] Optical techniques were employed to obtain the angular data and measure the photographic plates. A sample of the 1-D oscillatory motion is presented in Figure 3.

6

The results of the UNIVAC 1107 runs in applying the MDC to the experimental data showed the excellence of the data. This was indicated by a small probable error of "fit": the average was $.14^{\circ}$. This is an independent indication of the very small error in the angular measurement of the model motion. Also the values of the stability coefficients $C_{M_{\alpha}}$ and $(C_{M_q} + C_{M_{\dot{\alpha}}})$ were well determined. The average accuracy is 1% for $C_{M_{\alpha}}$ and 2% for $(C_{M_q} + C_{M_{\dot{\alpha}}})$.
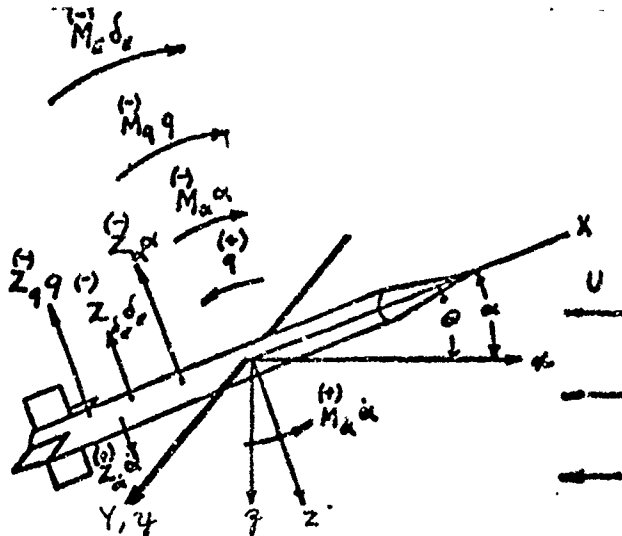
Figure 2. Force & Moment Diagram
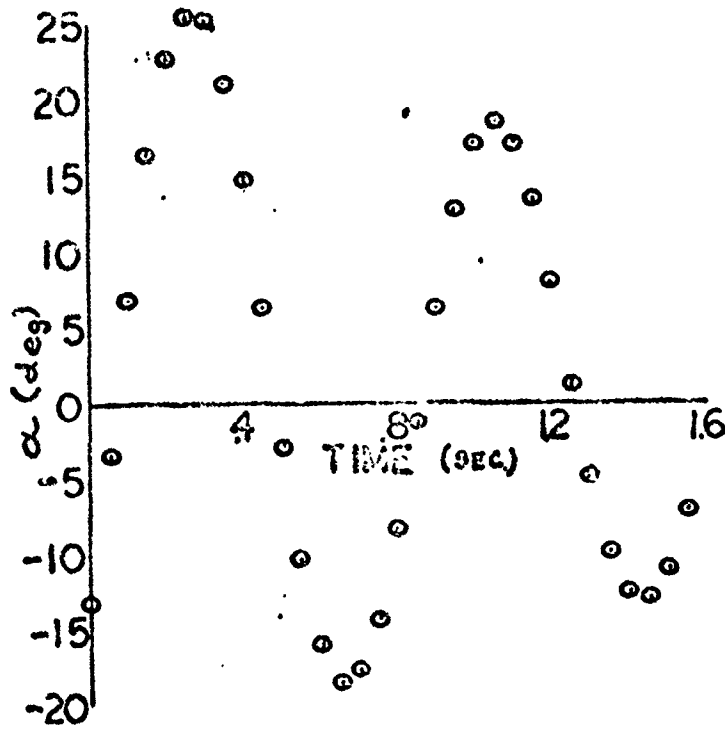
Figure 3. Angle of Attack versus Time

7

These moment stability derivatives are plotted in Figures 4 and 5 as a function of center of gravity position.

The static moment transformation equation, Equation (13), was fitted by least squares to the data in Figure 4. Also the damping moment transformation equation, Equation (14), was fitted by least squares to the data of Figure 5.

The P.E. of "fit" of the two transformation equations is of the same order as the accuracy of C_{M_α} and $(C_{M_q} + C_{M_{\dot\alpha}})$ in Table I. Thus the transformation relations were tested and found accurate. We have also obtained from the transformations the values for the force stability derivatives as in Table I.
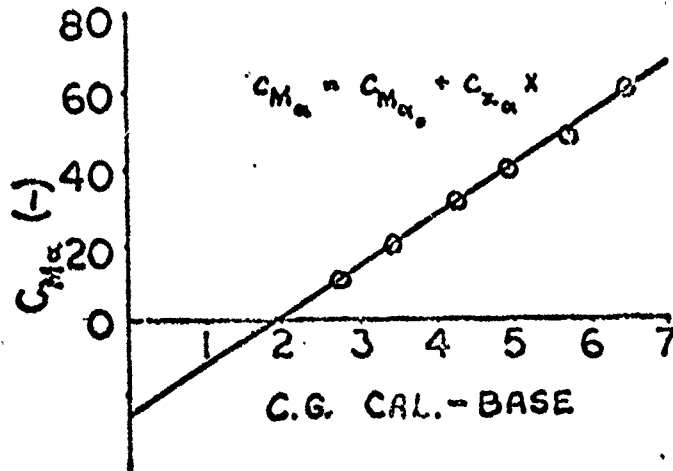
Figure 4. C_{M_α} versus C.G. Location
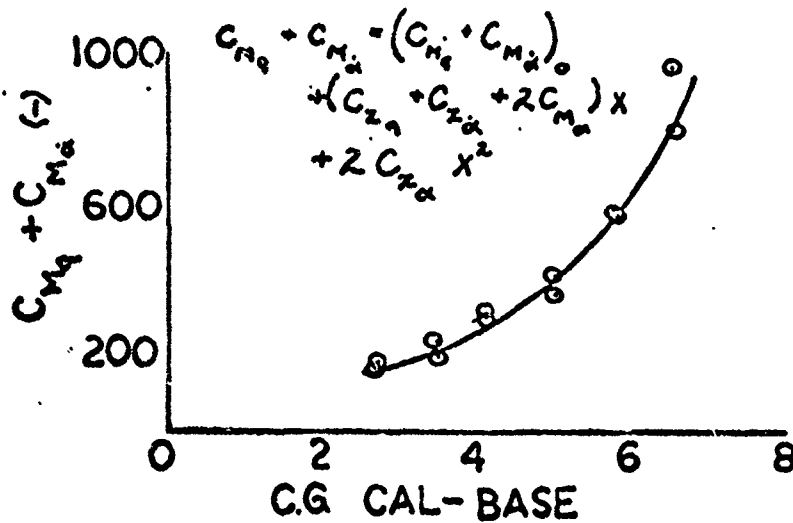
Figure 5. $C_{M_q} + C_{M_{\dot\alpha}}$ versus C.G. Location

8

TABLE I. TRANSFORMATION DATA

Static Moment Transformation   (C.G. = 5.0)

Coefficient	Value from Fit	Probable Error
$C_{M\alpha}$	-40.1	$\pm.168$
$C_{Z\alpha}$	-12.9	$\pm.126$
Probable Error of Fit	± 0.561	

Dynamic Moment Transformation Data

	Value	Probable Error
$C_{Mq} + C_{M\dot\alpha}$	-439.9	± 12.5
$C_{Zq} + C_{Z\dot\alpha}$	-120.3	± 9.4
Probable Error of Fit	± 41.75	

By applying MDC repeatedly to overlapping short sections of data, non-linearities in the stability coefficients may be studied. In Figures 6 and 7, the stability coefficients are plotted as functions of RMS α and RMS q . It is seen that $C_{M\alpha}$ and   ($C_{Mq} + C_{M\dot\alpha}$), and probably $C_{Z\alpha}$ and ($C_{Zq} + C_{Z\dot\alpha}$) are quite non-linear.
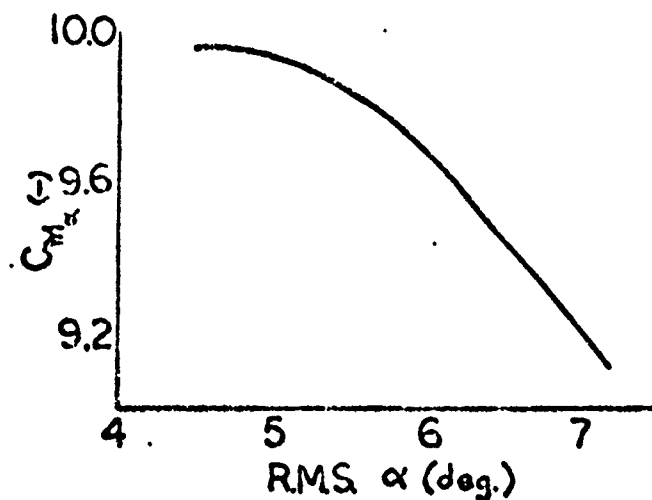
Fig. 6. $C_{M\alpha}$ versus RMS α
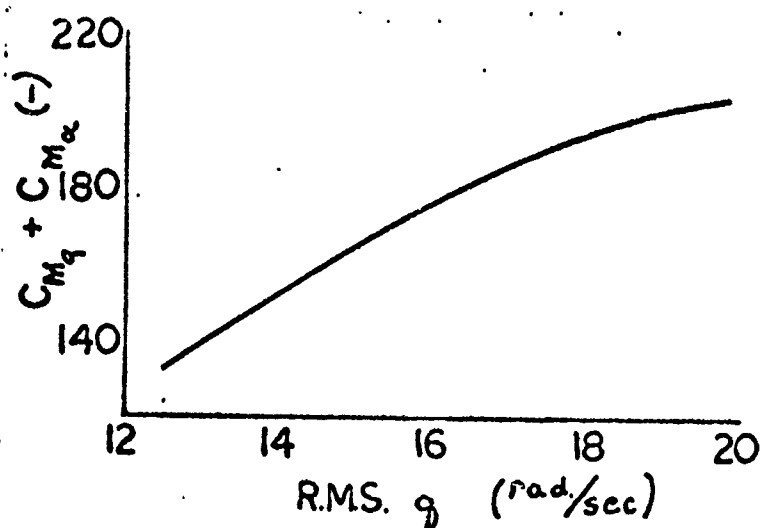
Fig. 7. $C_{M_q} + C_{M_{\dot{\alpha}}}$ versus RMS_q

Application of the linear theory to overlapping small sections of data gives only an indication of non-linearities in the aerodynamic stability coefficients. Therefore to determine more accurately these variations, a non-linear mathematical model must be utilized.

Non-Linear Analysis[7]

For the case where the stability coefficients are nonlinear functions of angle of attack as follows:

$$C_{M_q}(\alpha) = C_{M_{q_0}} + C_{M_{q_2}}\alpha^2 + \dots$$

$$C_{M_{\dot{\alpha}}}(\alpha) = C_{M_{\dot{\alpha}_0}} + C_{M_{\dot{\alpha}_2}}\alpha^2 + \dots \tag{15}$$

$$C_{M_\alpha}(\alpha) = C_{M_{\alpha_0}} + C_{M_{\alpha_2}}\alpha^2 + \dots$$

The approximate solution of the differential equation, Equation (6) is given as

$$\alpha = \alpha_T + K\cos(\omega t + \delta) \tag{16}$$

10

where, for quadratic variations in Equation (15),

$$K = 2K(0)\left\{(C_{M_q} + C_{M_{\dot\alpha}})_0 \Big/ \left[(C_{M_q} + C_{M_{\dot\alpha}})_2 K(0)^2 \times \left(1 - e^{\left(\frac{(C_{M_q} + C_{M_{\dot\alpha}})_2 QSD^2}{2IV}T\right)}\right)\right) + 4(C_{M_q} + C_{M_{\dot\alpha}})_0\right]\right\}^{\frac{1}{2}}$$
$$\times e^{\frac{(C_{M_q} + C_{M_{\dot\alpha}})_0 QSD^2}{4IV}} \quad ; \tag{17}$$

$$\omega = \sqrt{\frac{-C_{M_{\alpha_0}} QSD}{I}} - \frac{3}{8} C_{M_{\alpha_2}} \sqrt{\frac{IQSD}{-C_{M_{\alpha_0}}}} K^2 \tag{18}$$

$$a_T = \frac{-C_{M_{\delta_E}} \delta_E}{C_{M_{\alpha_0}} + \left[\frac{3}{2} C_{M_{\alpha_2}} + (C_{M_q} + C_{M_{\dot\alpha}})_2\right]} \tag{19}$$

Equation (16) may be fit to the angular data and Equations (17) to (18) then employed to obtain the non-linear variation of the stability coefficients with angle of attack. Figure 8 shows $C_{M_\alpha}(\alpha)$ to be non-linear and of a "soft-spring" nature. Figure 9 shows that $C_{M_q}(\alpha) + C_{M_{\dot\alpha}}\alpha$ also demonstrates non-linearity, but its variation is of a "hard spring" nature.

It has been shown[3,4,8] that for the case of a variable frequency ($C_{M_{\alpha_2}} \neq 0$ in the wind tunnel) the amplitude, K(t), must be corrected as follows

$$K_c(t) = K(t)\sqrt{\frac{\omega(t)}{\omega(0)}} \tag{20}$$

In order to examine the degree of accuracy of the approximate non-linear solution, numerical integrations of the equation of motion, Equation (6), were performed using a Fourth Order Runge Kutta scheme. Nominal values of the aerodynamic coefficients were input and the subsequent time history of $\alpha(t)$ was then fit[9] and the non-linear theory applied to the results. Table II shows the percent errors obtained from this analysis.

11

TABLE II. PERCENT ERROR FROM ANALYSIS

Coefficient	Input	Output	Percent Error
$C_{M_{\alpha_0}}$	-30.0	-29.94	0.18
$C_{M_{\alpha_2}}$	+15.0	+15.07	0.47
$(C_{M_q} + C_{M_{\dot\alpha}})_0$	-75.0	-74.83	0.21
$(C_{M_q} + C_{M_{\dot\alpha}})_2$	-50.0	-55.74	11.49
$C_{M_{\delta_e}} \delta_t$	1.0	1.0	0.

A model of the basic finner was mounted on a jewel support to minimize bearing friction in the angular oscillations.[7] Again, optical techniques were employed to determine the angular data. Several tests were conducted at one c.g. position to establish repeatability of the stability coefficients.

This dramatic difference in the nature of the non-linearities of these two important stability coefficients requires further study.

Of particular interest is the high degree of repeatability of the test runs. This fact provided added confidence in the application of the non-linear theory.

Fig. 8. C_{M_α} versus α

12
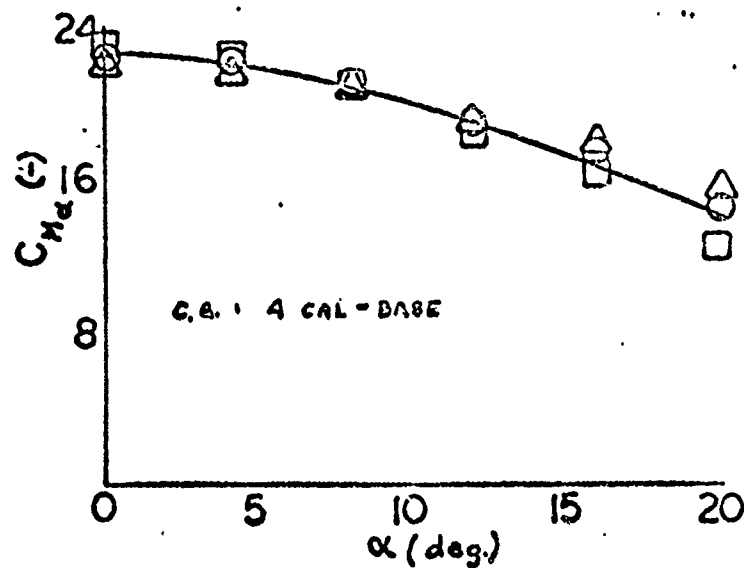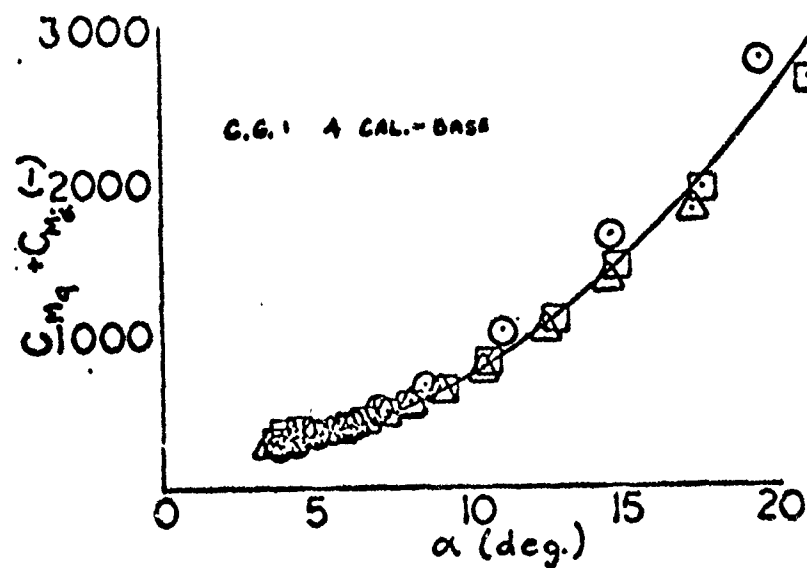
Fig. 9. $C_{Mq} + C_{M\dot{\alpha}}$ versus α

Mean values of the coefficients of the polynomial expression for the aerodynamic stability coefficients of Equation (15) are shown below.

$$\bar{C}_{M\alpha_0} = -22.65 \qquad\qquad \bar{C}_{M\alpha_2} = 68.31$$

$$(C_{Mq} + C_{M\dot{\alpha}})_0 = -193.58 \qquad\qquad (C_{Mq} + C_{M\dot{\alpha}})_2 = -19334.$$

These results suggest that the non-linear method of analysis should be used in order to obtain accurate values for the stability coefficients. It has been shown[4] that the "log - decrement" technique yields highly inaccurate results for the damping moment when the restoring moment is non-linear. Although use of Equation (20) tends to provide better results in this regard, it is strongly recommended that the complete non-linear method be employed.

13

SECTION IV

ROLL LOCK-IN[3]

It is well known that missiles and sounding rockets experiencing resonance instability have suffered abnormally large angles of attack unexplainable by resonance alone. This phenomena, known as Catastrophic Yaw[3], results from a lunar-type motion of the vehicle in the resonance region. This motion is characterized by the angle between a given fin and the (rotating) plane of the angle of attack being essentially constant, i.e. roll lock-in.[3] In order to more fully understand the effects and hopefully control roll lock-in, the simplified case of pure rolling motion at a constant angle of attack was first examined.

The governing equation for a rolling missile at constant angle of attack is

$$I_x \dot{P} = L(\delta_A) + L(P, \gamma, \alpha) + L(\gamma, \alpha)$$

where

$$L(\delta_A) = C_\ell(\delta_A) Q S d \qquad = \text{roll moment due to fin cant}$$

$$L(P, \gamma, \alpha) = C_\ell(P, \gamma, \alpha) Q S d = \text{roll damping moment}$$

$$L(\gamma, \alpha) = C_\ell(\gamma, \alpha) Q S d \qquad = \text{induced roll moment}$$

$$P = \dot{\gamma} \text{ for } \alpha = \text{constant.}$$

Theory and experiment have shown that the induced roll moment for a cruciform finned missile may be approximated by a sine function as

$$L(\gamma, \alpha) = L(\alpha) \sin 4\gamma$$

Therefore the differential equation of motion may be written

$$L(\delta_A) + L(P, \gamma, \alpha) + L(\alpha) \sin 4\gamma = I_x \ddot{\gamma} \qquad (21)$$

Linear Analysis

For the case where the roll damping moment is assumed to vary linearly with the rolling velocity and the inherent non-linear sine function approximated by a straight line tangent to the curve at the trim angle, Equation (21) may be written

14

$$L_{\delta A} \delta A + L_P(\alpha) \dot{\gamma} + \widetilde{L}_{\gamma \alpha} \gamma a = I_x \ddot{\gamma} \tag{22}$$

Since the coefficients of the differential equation are assumed constant, the solution for Equation (22) is the same as the solution for pitching motion discussed previously, and therefore we may write

$$\gamma_T = - \frac{C_{\ell_{\delta A}} \delta A}{C_{\ell_{\gamma a}} \gamma a} \tag{23}$$

$$\widetilde{C}_{\ell_{\gamma a}} = \frac{\omega^2 I_x}{QSd} \tag{24}$$

$$C_{\ell_P} = \frac{2 I_x \lambda}{\frac{d}{2V} QSd} \tag{25}$$

Two horizontal wind tunnel tests were conducted at supersonic speeds[10] to obtain a time history of γ for a Basic Finner exhibiting roll lock-in at a constant angle of attack. One test demonstrated damped roll oscillations while the other undamped. Figures 10 and 11 show the damped and the undamped oscillation respectively.
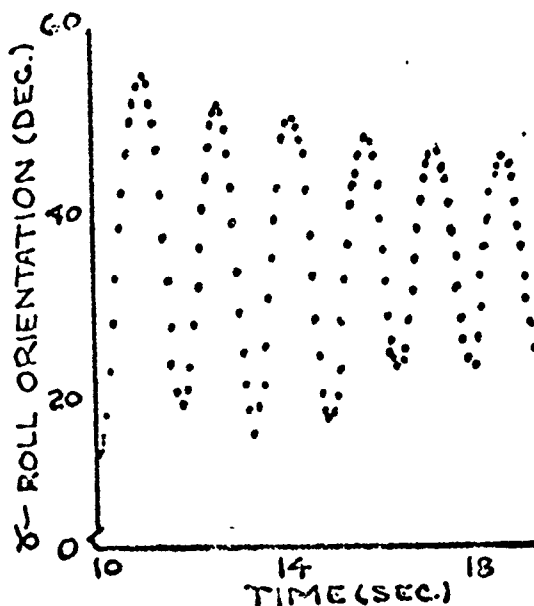
Figure 10. Roll Orientation versus Time

15
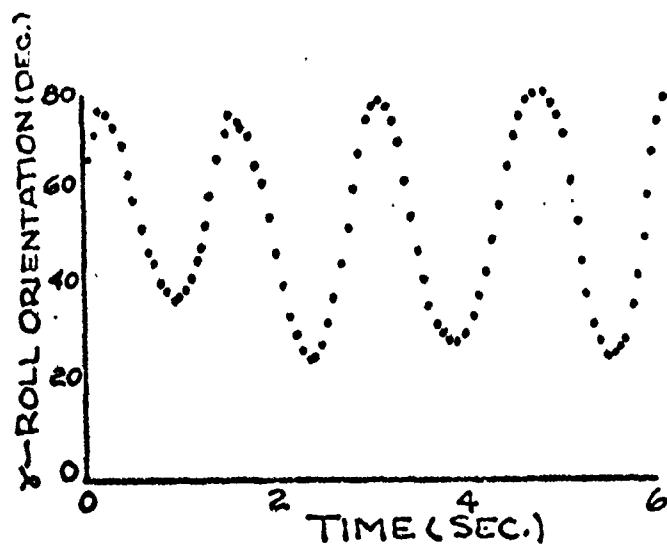
Figure 11. Roll Orientation versus Time

By fitting Equation (9) to the above angular data by the Method of Differential Corrections to obtain λ and ω, Equations (24) and (25) were used to compute C_{l_p} and $\widetilde{C}_{l_{\gamma\alpha}}$. These results are presented in Table III.

TABLE III. STABLE AND UNSTABLE ROLL COEFFICIENTS

Dynamic Stability	Mach No.	C_{l_p}	$\widetilde{C}_{l_{\gamma\alpha}}$
Stable	3.50	-6.66	-.027
Unstable	3.50	1.11	-.019

Non-Linear Analysis[11]

The first approximation of Kryloff and Bogoliuboff [12] was applied to the non-linear differential equation of motion, Equation (21),for the case of zero fin cant. While the induced roll moment term is inherently non-linear, the functional dependence of the roll damping moment, $L(p,\gamma,\alpha)$ on γ was also included.

By considering qualitatively the damping force distribution across the fins combined with the fin-body wake effect, the dependence of $L(p,\gamma,\alpha)$ on γ may be determined. As in the case of the linear analysis $L(p,\gamma,\alpha)$ was assumed to vary linearly with the rolling velocity.

16

$$L(p,\gamma,a) = L_p(\gamma,a)p = \left\{ L_{p_o}(a) + L_{p_2}(a)(\gamma - \frac{\pi}{4})^2 \right\}p \quad (26)$$
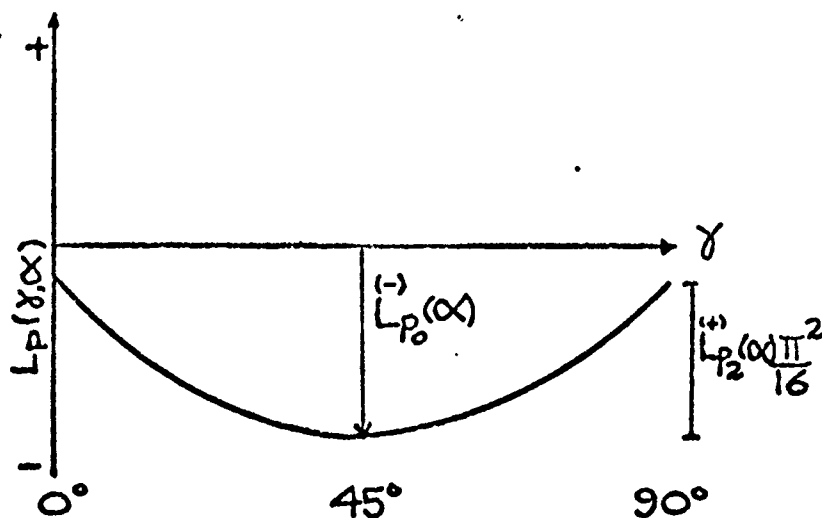
Figure 12. $L_p(\gamma,a)$ versus γ

Therefore the equation of motion may be written

$$\ddot{\gamma} - \frac{L_{p_o}(a)}{I_x}\dot{\gamma} - \frac{L_{p_2}(a)}{I_x}(\gamma - \frac{\pi}{4})^2\dot{\gamma} - \frac{L(a)}{I_x}SIN\,4\gamma = 0. \quad (27)$$

An approximate solution to the above non-linear equation is given as

$$\gamma = K\,COS(\omega t + \delta) \quad (28)$$

where

$$K = 2K(0)\left[C_{\ell_{p_o}} \Big/ (4C_{\ell_{p_o}} + C_{\ell_{p_2}}K(0)^2\left\{ 1 - e^{\frac{C_{\ell_n}QSd^2}{2I_xV}t} \right\})\right]^{1/2} e^{\frac{C_{\ell_{p_o}}QSd^2}{4I_xV}t} \quad (29)$$

$$\omega = \sqrt{\frac{C_\ell(a)QSd}{I_x}} + \frac{1}{2}\sqrt{\frac{QSd}{I_x}C_\ell(a)}\,\frac{J_1(4K)}{K} \quad (30)$$

17

In addition, the non-linear damping moment enabled the accurate prediction of a limit cycle in roll oscillation. The non-linear solution yields an equation for the time rate of change of the amplitude as follows

$$\frac{dK}{dt} = \frac{L_{P_0}}{2I_x}K + \frac{L_{P_2}}{8I_x}K^3$$

Hence, for a limit cycle

$$\frac{dK}{dt} = 0$$

and therefore

$$K = 2\sqrt{-C_{\ell_{P_0}}/C_{\ell_{P_2}}} = \text{constant} \qquad (31)$$

$$L_{P_0} < 0 \qquad L_{P_2} > 0$$

To investigate the accuracy of the limit cycle prediction, Equation (27) was numerically integrated with the linear and non-linear damping moments related to the initial amplitude as given by Equation (31). Results yielded roll oscillations which damped 0.25^O after 10 cycles of oscillation.

In addition, numerical studies were performed to substantiate the approximate non-linear solutions, Equations (28) to (30). The governing differential equation was numerically integrated to yield a time history of $\Upsilon(t)$. Equation (28) was then fit to these results by the Method of Differential Corrections and Equations (29) and (30) applied to compute $C_{\ell_{P_0}}$, $C_{\ell_{P_2}}$, $C_{\ell}(\alpha)$. The percent errors were computed with respect to the input values. A correction to the amplitude, similar to that of the 1-D pitching motion, must be applied due to the frequency variation. The results shown are for a damped roll lock-in oscillation with an initial roll angle of 70°. See Table IV.

TABLE IV. PERCENT ERROR OF COEFFICIENT COMPUTATION

Coefficient	Input	Output	% Error
$C_{\ell_{P_0}}$	-2.0	-2.02	1.00
$C_{\ell_{P_2}}$	15.0	14.42	3.87
$C_{\ell}(\alpha)$	0.5	.4998	.04

Subsonic wind tunnel tests are currently being undertaken to obtain aerodynamic data on the Basic Finner configuration from angular measurement of roll oscillations. A jewel support system mounted in a vertical

18

"blow-down" wind tunnel at the Aero-Space Engineering Department, University of Notre Dame, has drastically reduced the effect of bearing friction. At the present time calculations have been made to determine the induced roll moment coefficient at several angles of attack. The results shown below are for a basic finner model with flat plate fins.
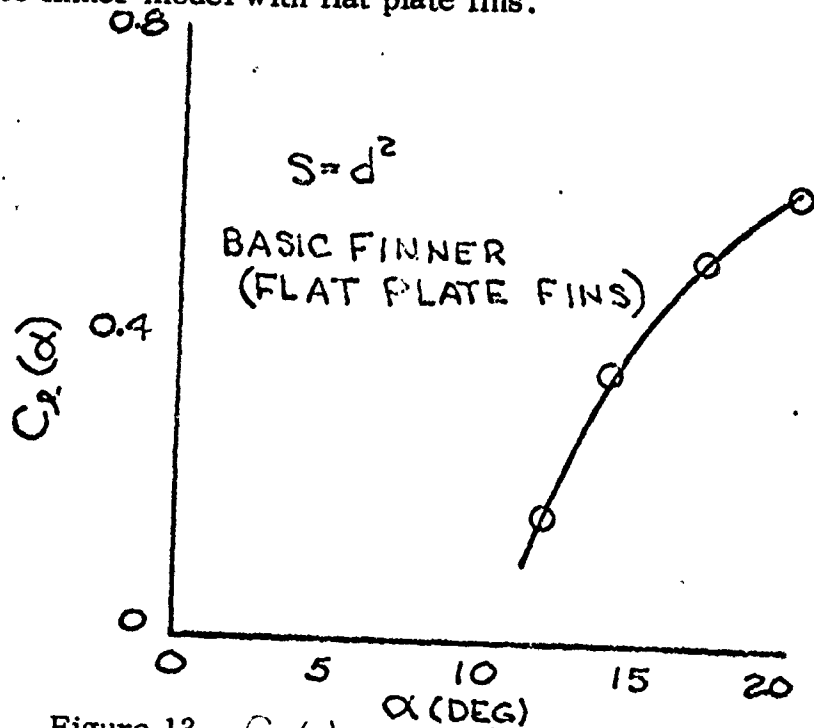
Figure 13. $C_\ell(\alpha)$ versus Angle of Attack

The variation of the induced roll moment coefficient with α compares favorably with that of Rhodes and Shannon [13] on cruciform-finned configurations. In addition, the data in Figure 13 demonstrates the possibility that $C_\ell(\alpha)$ may be negative for $\alpha \ll 3°$. This is also in agreement with the results obtained on other cruciform finned configurations. [13]

SECTION V

THREE DEGREE OF FREEDOM MOTION

A three degree of freedom pitching, yawing, and rolling model was designed for low subsonic dynamic wind tunnel testing. These tests included both a ball bearing side support system for use in a horizontal tunnel[14] and a jewel cup rear support system for use in a vertical "blow down" tunnel.[15] In the case of the side support, the entire model was free to roll except for a small cylindrical section at the center of gravity, while for the jewel support system no rolling constraints were applied.

Linear Analysis[3]

The differential equation for 3-D angular motion may be written as

$$M_\alpha \vec{\alpha} + M_{\mathfrak{z}} \dot{\vec{\alpha}} + M_{\dot\alpha} \dot{\vec{\alpha}} + i M_{P\alpha} P\alpha = I \ddot{\vec{\alpha}} - i P I_x \dot{\vec{\alpha}} \qquad (32)$$

The general solution when the coefficients are constant may be written as

$$\alpha = \vec{K}_1 e^{(\lambda_1 + i\omega_1)t} + \vec{K}_2 e^{(\lambda_1 + i\omega_1)t} + \vec{K}_3 e^{iPt} + \vec{K}_4 \qquad (33)$$

where

$$\lambda_{1,2} \simeq \left\{ \frac{(C_{M\mathfrak{z}} + C_{M\dot\alpha})}{2I} (1 \pm \tau) \pm \frac{C_{MP\alpha} \tau}{I_x} \right\} \frac{QSd^2}{2V} \qquad (34)$$

$$\omega_{1,2} \simeq \frac{PI_x}{2I} \left(1 \pm \frac{1}{\tau} \right) \qquad (35)$$

$$\tau = \frac{1}{(1 + \frac{1}{S})^{\frac{1}{2}}} \qquad S = \frac{P^2 I_x^2}{4I C_{M\alpha} QSd}$$

The aerodynamic coefficients may then be solved as

$$C_{M\alpha} = \frac{\omega_1 \omega_2 I}{QSd} \qquad (36)$$

20

$$C_{Mq} + C_{M\dot{\alpha}} = \frac{(\lambda_1 + \lambda_2)\, 2IV}{QSd^2} \tag{37}$$

$$C_{MP\alpha} = \frac{(\lambda_1 - \lambda_2)\, I_X V}{QSd^2 \tau} - \frac{C_{Mq} + C_{M\dot{\alpha}}}{2I} \tag{38}$$

These tests were directed towards an evaluation of the stability coefficients from 3-D angular motions with primary emphasis on obtaining $C_{MP\alpha}$

In a similar manner as for the 1-D pitching motion, optical techniques were employed to obtain the experimental 3-D angular data. An example of the complex angular motion is presented in Figure 14.
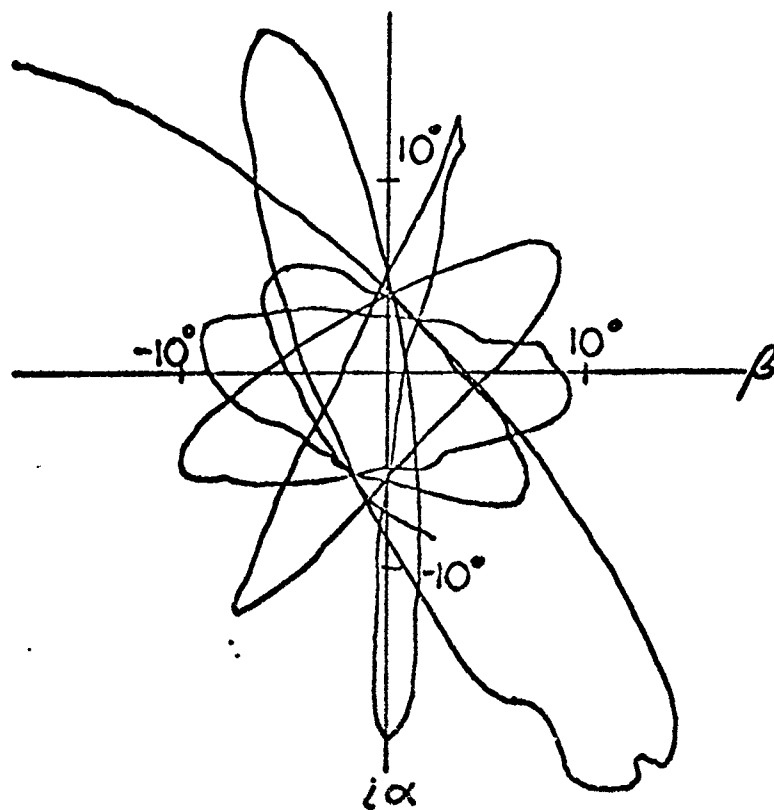
Figure 14. α versus β

By overlapping fits of small sections of data the motion parameters can be determined as continuous functions of time. The aerodynamic stability coefficients may then be determined from these motion parameters.

Sectional fits of Equation (33) to the above data resulted in a "probable error of fit" ranging from 0.5^O to 0.2^O as shown in Figure 15. The resulting mean percent error is approximately 2% to 3%.
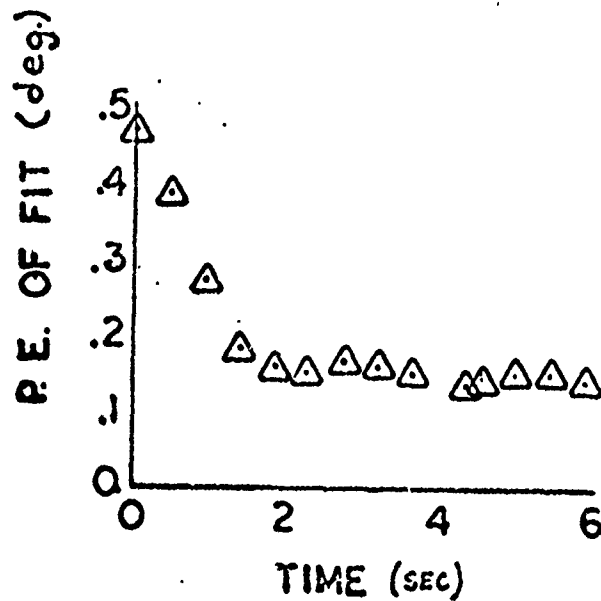
Figure 15. Probable Errors versus Time

The motion parameters obtained from sectional fits of the angular motion of Figure 14 are presented as functions of time in Figures 16 to 18.

It is seen from these results that small non-linear variations are present.

Using these motion parameters in addition to wind tunnel conditions and model mass parameters the stability coefficients C_{M_α} , $C_{M_q} + C_{M\dot\alpha}$, $C_{M_{p\alpha}}$ were computed from Equations (36), (37), and (38) respectively.

22
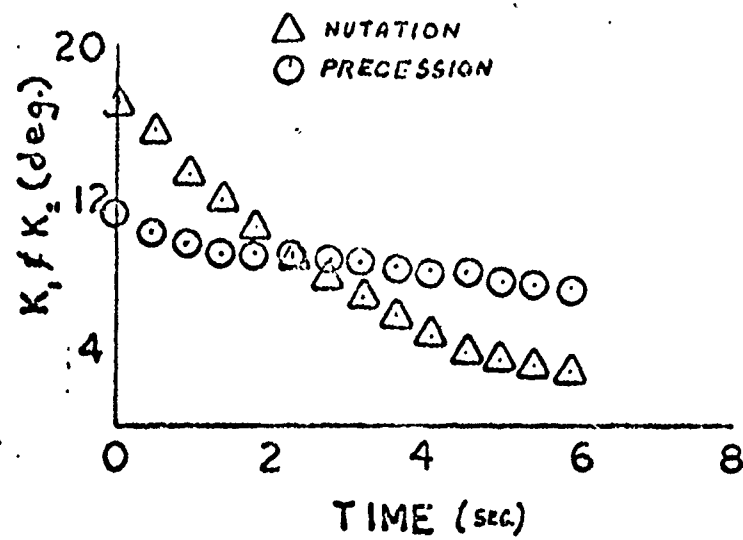
Figure 16. K_1 and K_2 versus Time
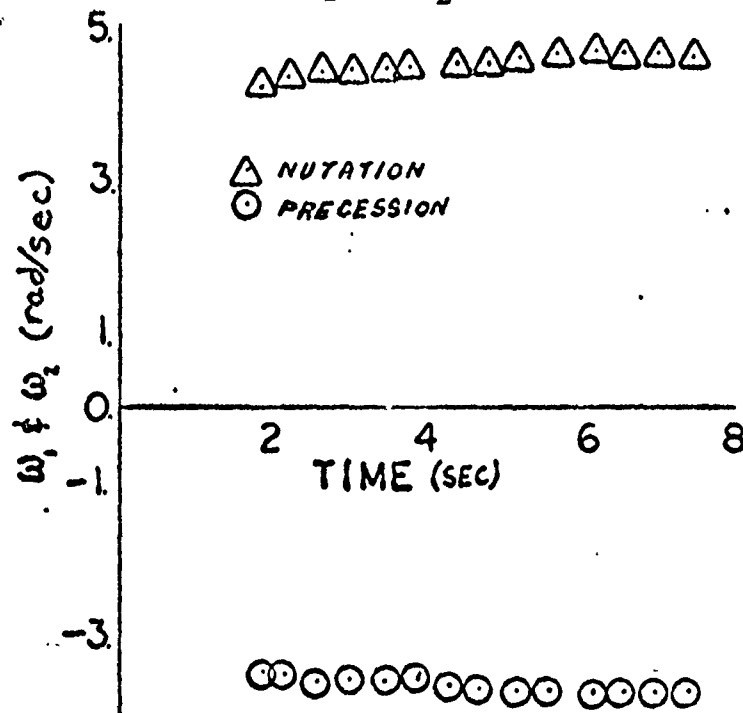
Figure 17. Frequencies versus Time

23
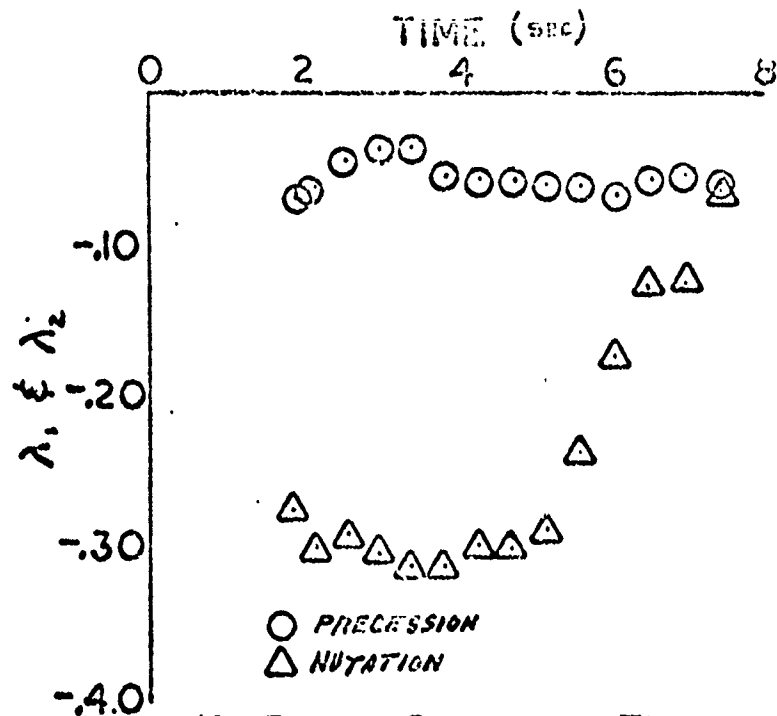
Figure 18. Damping Rates versus Time

The test runs were conducted at low subsonic speeds at one c.g. position.
Figures 19,20,21 present C_{M_α} , $C_{M_q} + C_{M_{\dot\alpha}}$, $C_{M_{p\alpha}}$ as a function of
mean angle of attack. The sectional fits yielded variations of the stability
coefficients with angle of attack which compare favorably with those obtained
from the 1-D linear and non-linear analyses.

Figure 19. C_{M_α} versus α

24
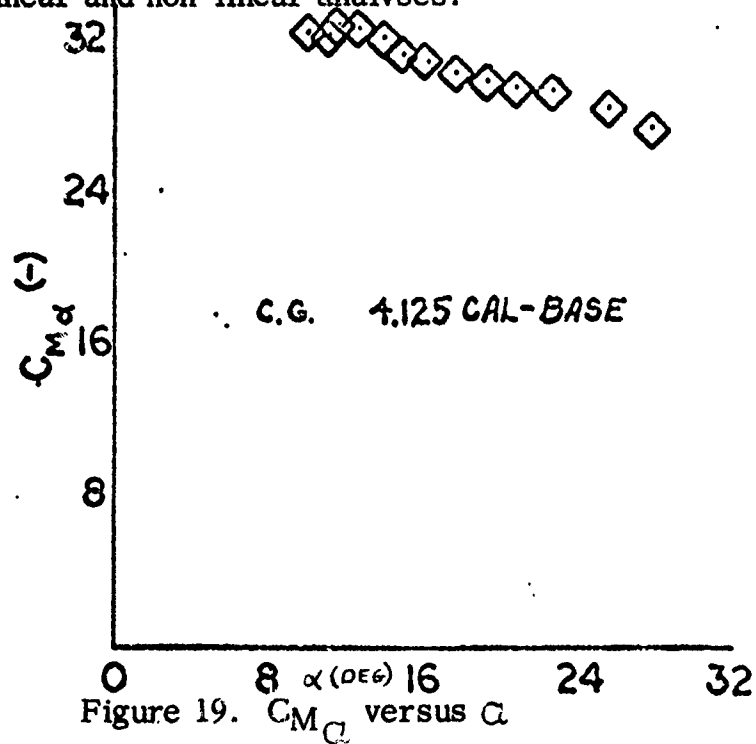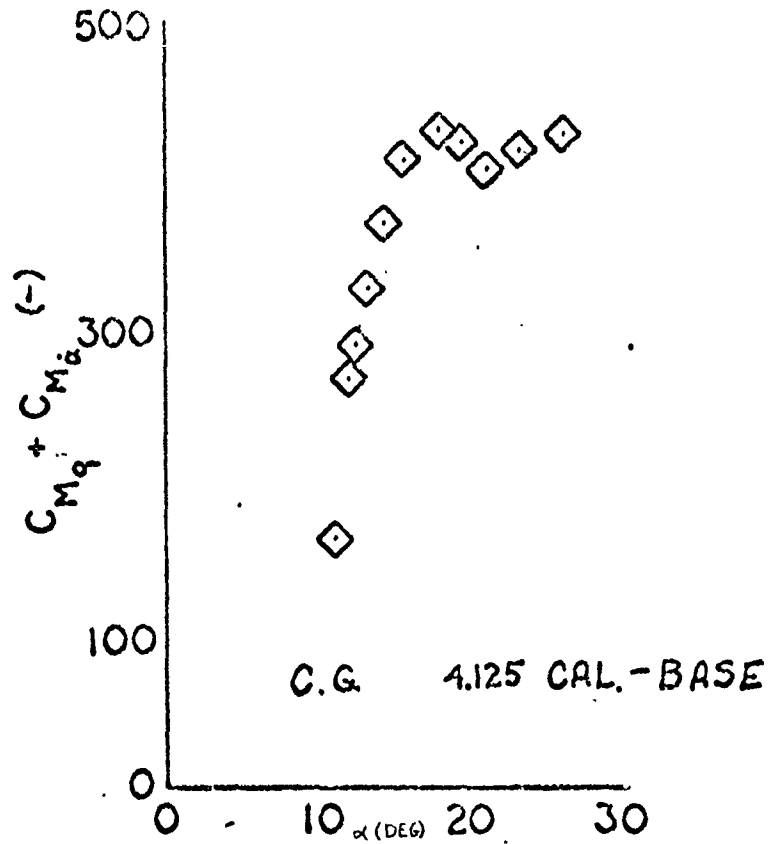
Figure 20. $C_{M_q} + C_{M_{\dot{\alpha}}}$ versus α
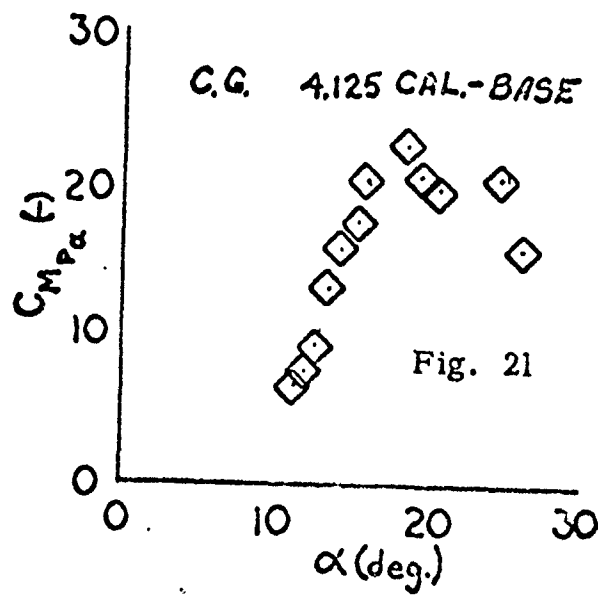
Figure 21. $C_{M_{p,\iota}}$ versus α

25

In addition, 3-D tests were conducted on a basic finner model mounted on a jewel sting support in the Notre Dame vertical "blow down" subsonic wind tunnel. The 3-D oscillations were obtained and reduced in a manner similar to that of the above analysis. It should be noted that this is a rear support, in contrast to the side support of the ball bearing system. This jewel system minimizes the bearing friction as well as reducing the support interference. The stability coefficients C_{M_α} and $C_{M_{p_\alpha}}$ obtained from several tests are presented in Figures 22 and 23. For the tests conducted, only the precession mode of oscillation was obtained. Hence, a value of $C_{M_q} + C_{M_{\dot\alpha}} = -350$ was used in determining the values of $C_{M_{p_\alpha}}$.
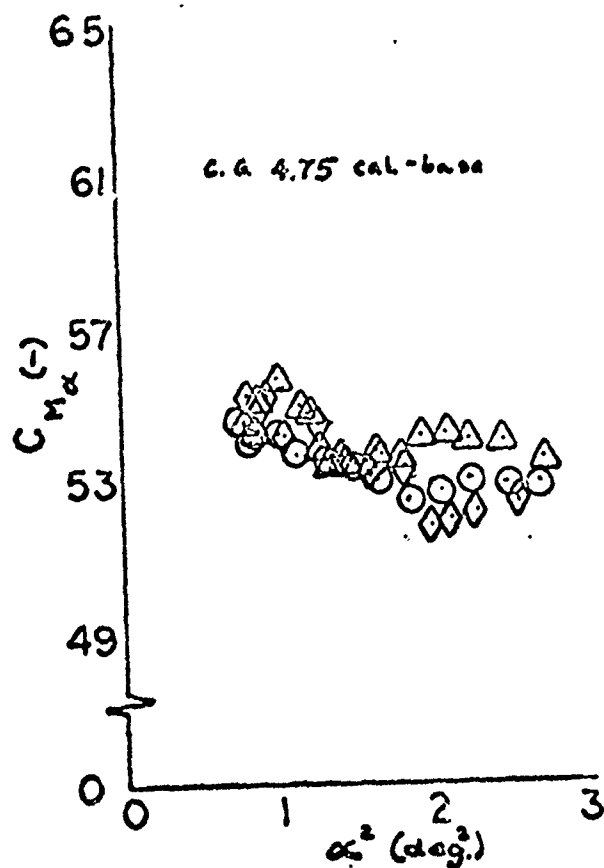
Figure 22. C_{M_α} versus α^2
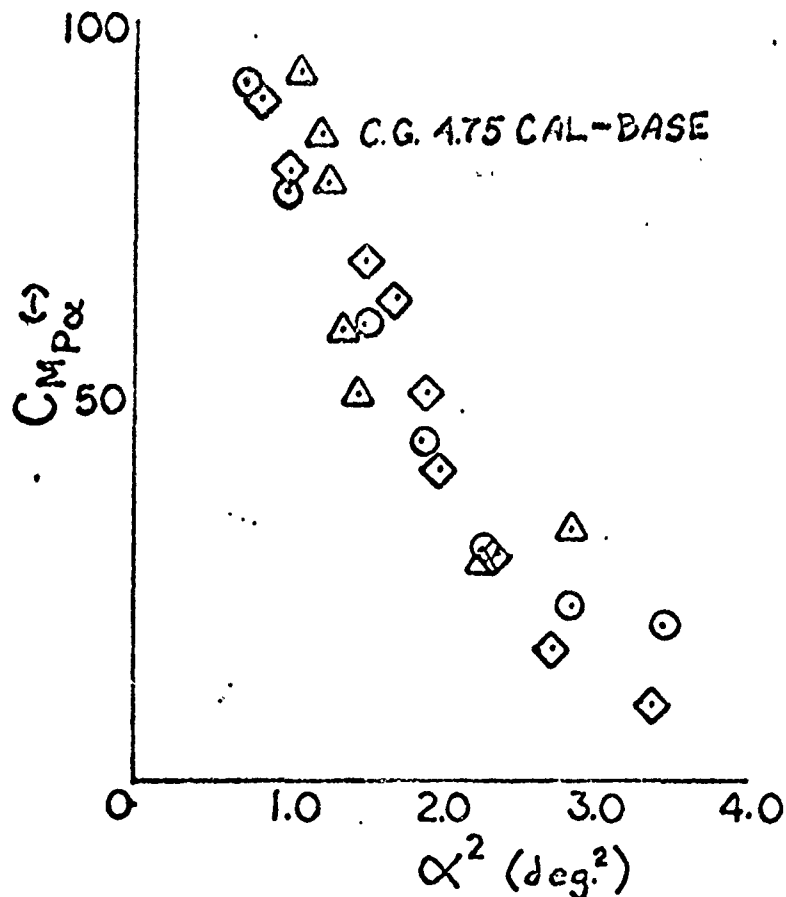
Figure 23. $C_{Mp\dot{\alpha}}$ versus α^2

In the comparison of $C_{M\alpha}$ it should be noted that the values in Figure 22 are larger than those of the previous 1-D and 3-D analyses. This results from the c.g. location in addition to the fact that the jewel supported model was equipped with roll tabs on the fins, thereby increasing the fin area by 12.5%.

The various stability coefficients of this linear analysis appear to vary with angle of attack. Thus it is essential to reconsider the solution of the equation of motion in which the stability coefficients are non-linear functions of the angle of attack.

Non-Linear Analysis[16]

For the case where the stability coefficients are non-linear functions of angle of attack

$$C_{M\alpha}(|\vec{a}|) = C_{M\alpha_o} + C_{M\alpha_2}|\vec{a}|^2 + \ldots$$

$$C_{M_g}(|\vec{a}|) = C_{M_{g_o}} + C_{M_{g_2}}|\vec{a}|^2 + \ldots$$

$$C_{M\dot{\alpha}}(|\vec{a}|) = C_{M\dot{\alpha}_o} + C_{M\dot{\alpha}_2}|\vec{a}|^2 + \ldots \tag{39}$$

$$C_{M_{P\alpha}}(|\vec{a}|) = C_{M_{P\alpha_o}} + C_{M_{P\alpha_2}}|\vec{a}|^2 + \ldots$$

an approximate solution for the complex angle of attack is given as

$$\vec{a} = \beta + i\alpha = K_1 e^{(\lambda_1 + i\omega_1)t} + K_2 e^{(\lambda_2 + i\omega_2)t} \tag{40}$$

where for quadratic variations in Equation (39),

$$\lambda_{1,2} = \frac{QSd^2}{2V}\left\{\frac{2IVC_{M\alpha_2}}{d(PI_x)^2}\,\tau_{1,2}(K_{1,2}^2\lambda_{1,2} + 2K_{2,1}^2\lambda_{2,1})\right.$$

$$+ \frac{(C_{M_g} + C_{M\dot{\alpha}})_o}{2I}(1 \pm \tau_{1,2}) + \frac{(C_{M_g} + C_{M\dot{\alpha}})_2}{2I}\left[(K_{1,2}^2 + K_{2,1}^2)\right.$$

$$\left.(1 \pm \tau_{1,2})\right] + K_{1,2}^2\,\tau_{1,2}\left(\frac{-1}{\tau_{2,1}} \pm 1\right) \pm \left. (C_{M_{P\alpha_o}} + C_{M_{P\alpha_2}}\delta_{E_{1,2}}^2)\right\} \tag{41}$$

$$\omega_{1,2} = \frac{PI_x}{2I}\left(1 \pm \frac{1}{\tau_{1,2}}\right) \tag{42}$$

$$\tau_{1,2} = \frac{1}{\sqrt{1 - \frac{1}{S_{1,2}}}} \tag{43}$$

$$S = \frac{P(I_x)^2}{4IQSd\left(C_{M_{\alpha_o}} + C_{M_{\alpha_2}}\delta_{E_{1,2}}^2\right)} \qquad (44)$$

$$\delta_{E_{1,2}} = K_{1,2}^2 + 2K_{2,1}^2 \qquad (45)$$

Since Equation (40) is an approximate solution, a numerical evaluation was conducted. Sample aerodynamic stability coefficients in the form of the quadratic variations in Equation (39) were input to a computer program which numerically integrates the 6-D equations of motion. A wind tunnel angular motion was simulated. Using the α and β output by the 6-D computer program, fits of the theory, Equation (40), were made to the angular data using the WOBBLE computer program to determine the stability coefficients. A comparison of the results obtained from the WOBBLE fits with those input to the 6-D program are given in Table V. As shown in these results, the approximate non-linear solution accurately represents the numerically integrated data.

This technique was applied to several tests of a particular 3-D of freedom cruciform-finned model at low subsonic velocities.[17] "Fits" of Equation (40) through (42) yields the non-linear aerodynamic stability coefficients. Figures 24 through 26 present the non-linear variation of C_{M_α}, $C_{M_q} + C_{M_{\dot\alpha}}$ and $C_{M_{p\alpha}}$ with angle of attack.

TABLE V. EVALUATION OF NON-LINEAR SOLUTION

Coef.	6-D Input	Wobble Output	% Error
$C_{M_{\alpha_o}}$	-113.	-113.	0
$C_{M_{\alpha_2}}$	1067.	1060.	0.7
$\left(C_{M_q}+C_{M_{\dot\alpha_o}}\right)$	-3000.	-3006.	0.2
$\left(C_{M_q}+C_{M_{\dot\alpha_2}}\right)$	49249.	50570.	2.7
$C_{M_{p\alpha_o}}$	1000.	1003.	0.3
$C_{M_{p\alpha_2}}$	16416.	15780.	3.9
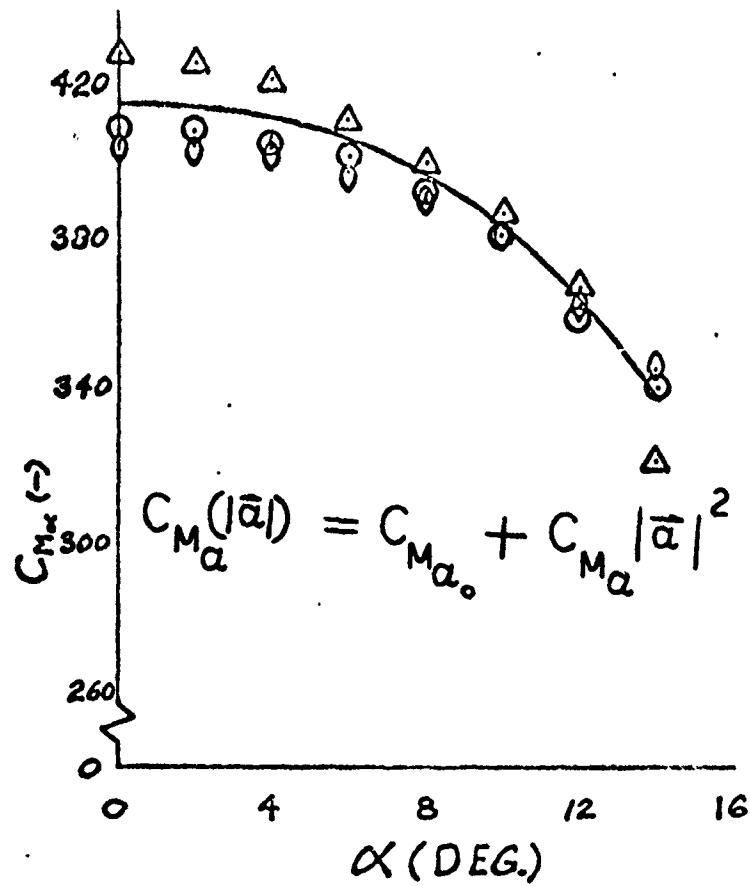
Figure 24. $C_{M\alpha}$ versus α

Mean values of the coefficients for the polynomial representation of the angle of attack variation of the stability coefficients were found to be

$$C_{M\alpha_0} = -412. \qquad C_{M\alpha_2} = 1122.$$

$$(C_{Mq} + C_{M\dot{\alpha}}) = -9154. \qquad (C_{Mq} + C_{M\dot{\alpha}})_2 = -212,633.$$

$$C_{Mp\alpha_0} = -577. \qquad C_{Mp\alpha_2} = 6469.$$

Figure 25. $C_{M_q} + C_{M\dot{\alpha}}$ versus α

The plot shows $-(C_{M_q} + C_{M\dot{\alpha}}) \times 10^{-2}$ on the vertical axis with values 10, 94, 118, 142, 168, 192, 216, 240 and α (DEG.) on the horizontal axis with values 0, 4, 8, 12, 16.

$$C_{M_q}(|\vec{\alpha}|) + C_{M_{\dot{\alpha}}}(|\vec{\alpha}|) =$$
$$\left(C_{M_q} + C_{M_{\dot{\alpha}}}\right)_0 + \left(C_{M_q} + C_{M_{\dot{\alpha}}}\right)_2 |\vec{\alpha}|^2$$

$$C_{M_{P\alpha}}(|\vec{\alpha}|) = C_{M_{P\alpha_0}} + C_{M_{P\alpha_2}}|\vec{\alpha}|^2$$
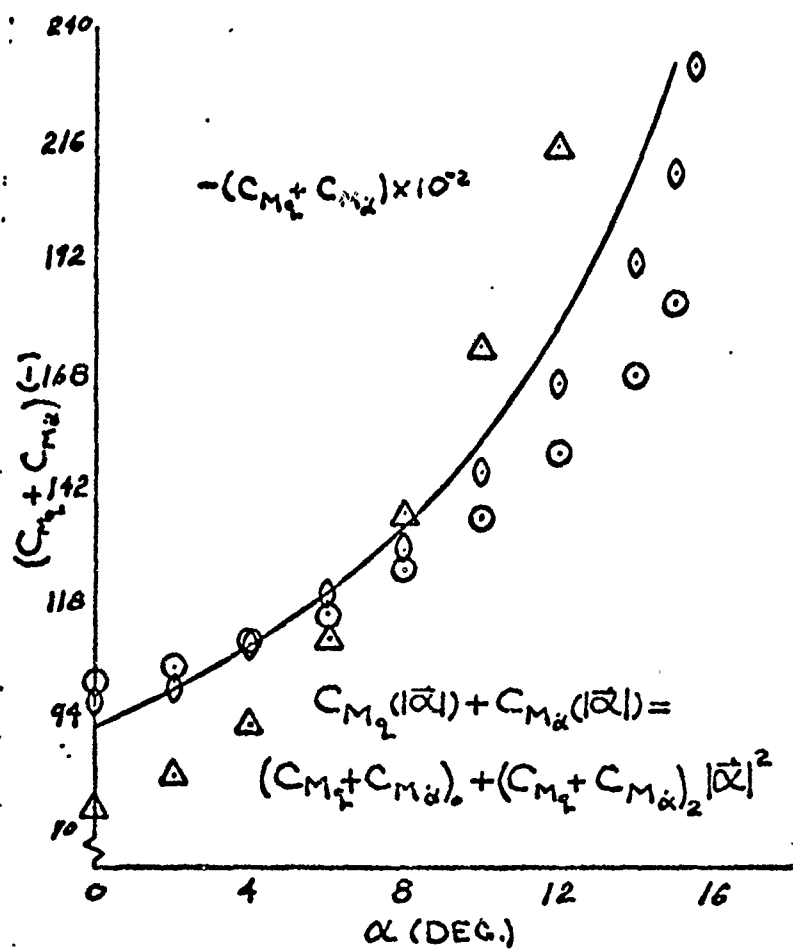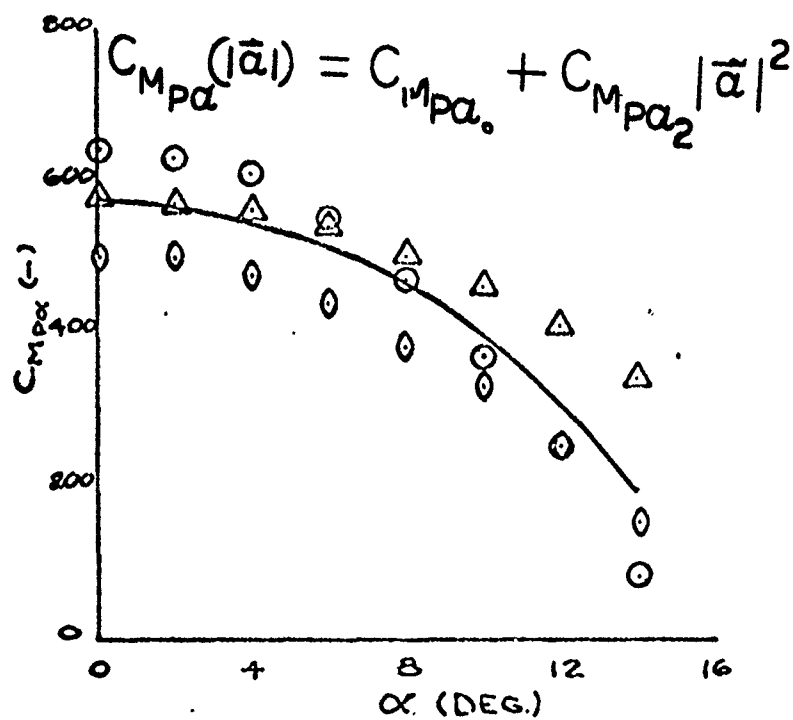
Figure 26. $C_{M_{p\alpha}}$ versus α

In analyzing the above results it is seen that the restoring moment exhibits "soft-spring" characteristics while, the damping moment shows a "hard spring" variation. This is the same trend as observed in the previous 1-D and 3-D results. Further study is required in this regard.

SECTION VI

CONCLUSIONS

Various non-linear methods of data analysis have been developed and evaluated by utilizing computer generated data and by comparing the results with the original inputs. In the case of the non-linear pure pitching motion, $C_{M\alpha}$ and ($C_{M_q} + C_{M\dot\alpha}$) agree to .18% and .21% respectfully, and the non-linear quadratic coefficients $C_{M\alpha_2}$ and ($C_{M_q} + C_{M\dot\alpha}$)$_2$ agree to .47% and 11.5%. In the case of the nonlinear pure rolling motion $C_{\ell_{P_0}}$ agrees to an accuracy of 1.0% and the non-linear quadratic coefficient $C_{\ell_{P_2}}(\gamma^2)$ and $C_\ell(\alpha)$ agree to 3.87% and .04% respectfully. In the case of combined pitching, yawing and rolling motion $C_{M\alpha}$ and ($C_{M_q} + C_{M\dot\alpha}$) agree to .01% and .2%. The non-linear coefficients $C_{M\alpha_2}$ and ($C_{M_q} + C_{M\dot\alpha}$)$_2$ agree to .7% and 2%. Of particular importance is the Magnus coefficient $C_{M_{P\alpha}}$ which agrees to .3% and the non-linear quadratic Magnus coefficient, $C_{N_{P\alpha_2}}$ which agrees to 3.9%.

Various new dynamic wind tunnel testing techniques were developed and the data was reduced by using the new non-linear methods of analysis. The experimental data was found to be well represented by the theories for the three non-linear motions considered: pure pitching, pure rolling and combined pitching, yawing, and rolling. The values for the associated stability coefficients $C_{M\alpha}$, ($C_{M_q} + C_{M\dot\alpha}$), $C_{M_{P\alpha}}$ and $C_\ell(\alpha)$ compare well in repeated tests and the detailed results are all represented. It is concluded that the various motions are definitely non-linear and that the non-linear methods must be used for their reduction and analysis. It is suggested that previous disagreement between data from various facilities may be due to these serious non-linear effects.

For the Basic Finner configuration it is found that the non-linear restoring moment is of the "soft-spring" type while the non-linear damping and lag moments are of the "hard spring" type. Future study is suggested in this area.

Of particular importance are the new dynamic wind tunnel testing techniques utilizing special jewel supports which permit nearly frictionless free motion. The unique vertical "downdraft" wind tunnel has yielded excellent data on pure rolling motion and on combined pitching, yawing, and rolling motions.

33

(The reverse of this page is blank)

REFERENCES

1. Bolz, R.E., and Nicolaides, J.D., A Method of Determining Some Aerodynamic Coefficients from Supersonic Free-Flight Tests of a Rolling Missile, Journal of the Aeronautical Sciences, Vol. 17, No. 10, Oct., 1950, BRL Rept. No. 711.

2. Nicolaides, J.D., On the Free Flight Motion of Missiles Having Slight Configurational Asymmetries, BRL Rept. No. 858, 1953, and IAS Preprint No. 395, 1952.

3. Nicolaides, John D., Free Flight Dynamics, Text, Aero-Space Engineering Department, University of Notre Dame, 1961.

4. Eikenberry, R., Wobble, Analysis of Missile Dynamic Data, Part I: Angular Motion, Aero-Space Engineering Department, University of Notre Dame, 1967.

5. Nelson, R.C., On the Pure Pitching Motion of the Basic Finner Missile, Master's Thesis, Department of Aero-Space Engineering, University of Notre Dame, 1966.

6. Nicolaides, John D., Eikenberry, R.S., Dynamic Wind Tunnel Testing Techniques, AIAA Aerodynamic Testing Conference, Los Angeles, California, 1966.

7. Clare, T.A., Chin, A.B., Lando, D.W., A Technique for Obtaining Non-Linear Aerodynamic Stability Coefficients for a Missile Pure Yaw, Aero-Space Engineering Department Report, University of Notre Dame, 1968.

8. Murphy, C., Free Flight Motion of Symmetric Missiles, BRL Report No. 1216, Aberdeen Proving Ground, Maryland, 1963.

9. Clare, T.A., FIT, A Program to Fit Analytic Functions to Data by Differential Corrections, Aero-Space Engineering Department Report, University of Notre Dame, 1968.

10. Bozzonetti, E., Analysis of the Oscillating Motions Associated with Roll Lock-In, Master's Thesis, Department of Aero-Space Engineering, University of Notre Dame, 1966.

11. Clare, T.A., A Non-Linear Analysis of Dynamic Roll Lock-In in One Degree of Freedom, Aero-Space Engineering Department Report, University of Notre Dame, 1968.

12. Klyloff, N., Bogolinhoff, N., Introduction to Non-Linear Mechanics, Translated by S. Lefschetz, Princeton Univ. Press, Princeton, New Jersey, 1947.

13. Rhodes, C.W., Shannon, J.H.W., Results and Conclusions of the Joint R.A.E./W.R.E. Research Programme on the Flight Dynamics and Ballistic Consistency of Freely Falling Missiles, Part I: Bombs Stabilized by Fixed Cruciform Fins, Department of Supply, Australian Defense Scientific Service, Weapons Research Establishment, HSA 20, 1965.

14. Lorenzen, C., On the Determination of the Magnus Moment Coefficient for the Basic Finner, Master's Thesis, Department of Aero-Space Engineering, University of Notre Dame, 1967.

15. Foust, J., On the Investigation of a Vertical Wind Tunnel System for Determining Aerodynamic Moment Coefficients, Master's Thesis, Department of Aero-Space Engineering, University of Notre Dame, 1968.

16. Ingram, C., An Approximate Solution of the Non-Linear Differential Equation for the Complex Angle of Attack of a Symmetric Missile, Air Proving Ground Center, Eglin Air Force Base, Florida. (Pending Publication).

17. Ingram, C., Martin, J., A Three Degree of Freedom Subsonic Wind Tunnel Test of the Apache Sounding Rocket, White Sands Missile Range, New Mexico (Pending Publication).

18. Nicolaides, Eikenberry, Ingram and Clare, On the Flight Dynamics of the Basic Finner in Various Degrees of Freedom. AIAA Paper No. 68-890.

DOCUMENT CONTROL DATA - R & D

(Security classification of title, body of abstract and indexing annotation must be entered when the overall report is classified)

1 ORIGINATING ACTIVITY (Corporate author)	2a. REPORT SECURITY CLASSIFICATION
Department of Aero-Space Engineering University of Notre Dame Notre Dame, Indiana	UNCLASSIFIED
	2b. GROUP

3 REPORT TITLE

FLIGHT DYNAMICS OF THE BASIC FINNER IN VARIOUS DEGREES OF FREEDOM

4. DESCRIPTIVE NOTES (Type of report and inclusive dates)

Final Report - February 1966 to May 1968

5. AUTHOR(S) (First name, middle initial, last name)

John D. Nicolaides   Charles W. Ingram
Robert S. Eikenberry   Thomas A. Clare

6. REPORT DATE	7a. TOTAL NO. OF PAGES	7b. NO. OF REFS
July 1968	45	17

8a. CONTRACT OR GRANT NO.	9a. ORIGINATOR'S REPORT NUMBER(S)
AF 08 (635)-5275	
b. PROJECT NO.	
c.	9b. OTHER REPORT NO(S) (Any other numbers that may be assigned this report)
d.	AFATL-TR-68-82

10. DISTRIBUTION STATEMENT

This document is subject to special export controls and each transmittal to foreign governments or foreign nationals may be made only with prior approval of the Air Force Armament Laboratory (ATPR), Eglin AFB, Florida 32542.

11. SUPPLEMENTARY NOTES	12. SPONSORING MILITARY ACTIVITY
Available in DDC	Air Force Armament Laboratory Air Force Systems Command Eglin Air Force Base, Florida

13. ABSTRACT

Basic Finner models are tested in both horizontal and vertical wind tunnels in order to develop dynamic testing techniques and to perfect new methods of non-linear analysis. The simple free motions of pure pitching and pure rolling are first studied. Then, free angular motions of combined pitching, yawing, and rolling are investigated. While the linear analysis methods appear to yield good results, the new non-linear analysis methods are found to be essential in providing an accurate representation of the various motions and in providing correct values for the various static and dynamic stability coefficients. ( )

DD FORM 1 NOV 65 1473

14. KEY WORDS	LINK A		LINK B		LINK C	
	ROLE	WT	ROLE	WT	ROLE	WT
Flight Dynamics						
Basic Finner						
Degrees of Freedom						
Non-Linear Analysis						
Linear Analysis						